Published in final edited form as:
Cell Rep. 2012 August 30; 2(2): 223–230. doi:10.1016/j.celrep.2012.07.001.

Target-Derived Matricryptins Organize Cerebellar Synapse Formation Through α3β1 Integrins

Jianmin Su[1], **Renee S. Stenbjorn**[1], **Karen Gorse**[1], **Kaiwen Su**[1], **Kurt F. Hauser**[2], **Sylvie Ricard-Blum**[3], **Taina Pihlajaniemi**[4,5,6], and **Michael A. Fox**[1]

[1]Department of Anatomy and Neurobiology, Virginia Commonwealth University Richmond, VA 23298 USA [2]Department of Pharmacology and Toxicology Virginia Commonwealth University Richmond, VA 23298 USA [3]Institut de Biologie et de Chimie des Protéines UMR 5086 CNRS, University Lyon 1 France [4]Oulu Center for Cell-Matrix Research, 90014 University of Oulu Finland [5]Biocenter Oulu, 90014 University of Oulu Finland [6]Department of Medical Biochemistry and Molecular Biology 90014 University of Oulu Finland

SUMMARY

Trans-synaptic organizing cues must be passed between synaptic partners for synapses to properly form. Much of our understanding of this process stems from studies at the neuromuscular junction (NMJ) where target-derived growth factors, extracellular matrix (ECM) molecules, and matricryptins (proteolytically released fragments of ECM molecules) are all essential for the formation and maintenance of motor nerve terminals. While growth factors and ECM molecules also contribute to the formation of brain synapses, it remains unclear whether synaptic roles exist for matricryptins in the mammalian brain. Here, we report collagen XVIII, and its matricryptin endostatin, are generated by cerebellar Purkinje cells and are necessary for the organization of climbing fiber terminals onto these neurons. Moreover, endostatin is sufficient to induce climbing fiber terminal formation *in vitro* by binding and signaling through α3β1 integrins. Taken together, these studies reveal novel roles for both matricryptins and integrins in the organization of brain synapses.

INTRODUCTION

Synapses, which allow the transfer of information between cells in the nervous system, begin to form when growing axons contact appropriate target cells. After initial contact molecular signals are passed between synaptic partners to transform the axon and postsynaptic target into a synapse. First insight into the molecular signals that mediate this process (termed synaptic differentiation) came from studies at the neuromuscular junction (NMJ), where trans-synaptic cues, in the form of growth factors, morphogens, and extracellular matrix (ECM) molecules, induce pre- and postsynaptic differentiation (Fox and Umemori 2006). Recent studies have further demonstrated that proteolytically released fragments of ECM molecules also contribute to NMJ formation (Fox et al. 2007).

Corresponding Author: Michael A. Fox 1101 East Marshall Street, Richmond, VA 23298-0709 Phone: (804) 628-3001 Fax: (804) 828-9477 mafox@vcu.edu.

Specifically, controlled proteolysis of several collagen molecules generates soluble peptides, termed matricryptins, that exhibit unique bioactivities compared to the full-length molecule from which they are derived (Ricard-Blum and Ballut 2011). At the NMJ, collagen IV-derived matricryptins direct the assembly and maintenance of motor nerve terminals (Fox et al. 2007).

Despite anatomical differences, the formation of central synapses is remarkably similar to that of the NMJ in that trans-synaptic cues direct synaptic differentiation (Fox and Umemori 2006). In fact, many of the same families of molecules that direct NMJ formation contribute to synapse formation in the brain. Examples include Wnts, FGFs, agrin and laminins (Terauchi et al. 2010; Ksiazek et al. 2007; Egles et al. 2007). It remains unclear, however, whether roles for matricryptins exist at central synapses. Here, we screened for matricryptin-releasing collagens in brain and discovered that cerebellar Purkinje cells express collagen XVIII. Using *in vivo* and *in vitro* approaches we show that collagen XVIII is necessary for the organization of climbing fiber terminals, and endostatin – the matricryptin released from this collagen – is sufficient to induce their formation.

RESULTS AND DISCUSSION

Matricryptin expression in cerebellum

To assess whether matricryptins are present in the mammalian brain we screened for collagen gene expression in mouse brain. One collagen gene - *col18a1* (which encodes collagen XVIII) - was exclusively enriched in cerebellum (Fig. 1A). Outside of the nervous system 3 *col18a1* isoforms are expressed in tissue-specific manners (Muragaki et al. 1995) however we found that all were expressed in cerebellum (Fig. S1A,B). Using primers and riboprobes that detect all *col18a1* isoforms we found that expression coincides with synaptogenesis (Fig. 1B) and is restricted to a single class of neurons – Purkinje cells (Fig. 1C,D and S1C).

Collagen XVIII is a heparan sulfate proteoglycan and harbors a C-terminal matricryptin termed endostatin. Outside of the nervous system endostatin shares functional similarities with those collagen IV-derived matricryptins that organize NMJ formation (Ricard-Blum and Ballut 2011). In addition to these similarities with synaptogenic matricryptins, endostatin was a good candidate to direct synaptogenesis in the mammalian brain since it regulates neuromuscular circuit formation in worms, flies and fish (Ackley et al. 2003, Meyer et al. 2009, Schneider and Granato 2007). We therefore asked whether endostatin contributes to cerebellar circuit formation.

To answer this question we began by assessing whether endostatin protein was present in cerebellum. Western blots with an antibody that specifically react with the endostatin domain of collagen XVIII revealed 2 endostatin-containing peptides (~20 and 25 kDa) were present in cerebellum (Fig. 1E). These fragments were absent from other brain regions and from cerebellum of mice lacking collagen XVIII (*col18a1*$^{-/-}$)(Fig. 1E,F). Similar to mRNA levels, increases in endostatin levels coincided with synaptogenesis (Fig. 1G). Unfortunately anti-endostatin antibodies worked poorly for localizing this matricryptin in brain tissue. To circumvent this problem, we probed for endostatin in cerebellar synaptosomes – biochemical fractions enriched for synaptic elements. A single 20kDa endostatin-containing fragment appeared present in cerebellar synapses (Fig. 1H and S1D), suggesting that cleavage of endostatin from collagen XVIII may be different in synaptic and extrasynaptic compartments of the cerebellum. Together these results demonstrate that Purkinje cells not only generate collagen XVIII/endostatin during synapse formation but endostatin is present at cerebellar synapses.

Collagen XVIII/endostatin is necessary for climbing fiber terminal formation

Based on the role of matricryptins at the NMJ, we hypothesized that endostatin may be necessary to organize nerve terminal assembly onto Purkinje cell dendrites. Nerve terminals from four types of neurons synapse onto Purkinje cells: parallel fibers (PFs), which originate from granule cells, form excitatory terminals onto dendritic spines of Purkinje cell dendrites; basket cells (BCs) form inhibitory terminals onto the Purkinje cell soma and axon initial segment; stellate cells (SCs) form inhibitory terminals onto Purkinje cell dendrites; climbing fibers (CFs) originate from inferior olivary neurons and form excitatory terminals on the proximal shaft of Purkinje cell dendrites (Fig. 2A) (Sotelo 2008). Since there is no method to eliminate matricryptins without affecting full-length collagen (because of the necessity of C-terminal matricryptins for collagen trimerization within the ER), we assessed synapses in *col18a1*$^{-/-}$ mutants which lack both collagen XVIII and endostatin. These mutants are viable and have morphologically normal cerebella (Fig. S2).

To visualize different subsets of nerve terminals on Purkinje cell dendrites, we immunostained cerebellar tissue with antibodies directed against distinct isoforms of nerve terminal associated proteins (Fig. 2B). PF terminals were labeled with antibodies against vesicular glutamate transporter 1 (VGluT1) or Bassoon (Fremeau et al. 2001; Richter et al. 1999). To label inhibitory terminals, we used antibodies against synaptotagmin 2 (Syt2), a synaptic vesicle-associated protein expressed by interneurons within the cerebellar molecular layer (and in a population of PF terminals) (Fig. 2B, S3, S4)(Fox and Sanes 2007). We detected no remarkable difference in the density or distribution of VGluT1, Bassoon, or Syt2 in *col18a1*$^{-/-}$ mutants or littermate controls (Fig. 2C-K). Lastly, to label CF terminals antibodies against VGluT2 were employed (Fremeau et al. 2001)(Fig. 2B and S4). We observed a dramatic and statistically significant decrease in the number of VGluT2-containing varicosities in the molecular layer of mutant cerebella (Fig. 2L-N). Not only were fewer VGluT2-rich varicosities observed, but VGluT2 appeared diffusely distributed throughout mutant CFs rather than being aggregated into distinct varicosities (Fig. 2L,M). The abnormal distribution of VGluT2, together with little change in its expression pattern (Fig. 2O,P), suggested that collagen XVIII/endostatin is critical for the clustering of presynaptic elements into nerve terminals, a hallmark feature of presynaptic differentiation. Based on these defects in synaptic organization, we asked whether *col18a1*$^{-/-}$ mutants exhibit motor dysfunction in a standard accelerating rotarod test (Shiotsuki et al. 2010). *Col18a1*$^{-/-}$ mutants performed significantly worse than controls in this assay (Fig. 2Q), a phenotype that suggests (but does not prove) cerebellar defects.

Based upon the organizing role of collagen-derived matricryptins at the NMJ, we hypothesized that reduced numbers of VGluT2-containing CF terminals and motor deficits in *col18a1*$^{-/-}$ mutants arose as a result of endostatin's role in inducing presynaptic differentiation. However, CFs initially arborize around the Purkinje cell somas and then subsequently “climb” the proximal shaft of Purkinje cell dendrites (Mason and Gregory 1984). Therefore, an alternative possibility was that synaptic defects in *col18a1*$^{-/-}$ mutants arose indirectly due to defects in Purkinje cell dendritogenesis or CFs ability to ascend these dendrites. To explore these possibilities, we performed morphological characterizations of Purkinje cell dendrites and CF arbors. Purkinje cell dendrites were labeled by Golgi impregnation – a method in which a small percentage of cerebellar cells were labeled stochastically (Fig. S2E,F). Areas occupied by individual Purkinje cell dendrites and branch densities of these dendrites appeared indistinguishable in mutant and control cerebella (Fig S2G,H).

To address whether CFs properly contacted and ascended Purkinje cell dendrites in *col18a1*$^{-/-}$ mutants we explored whether CF terminals formed onto Purkinje cells in mutants. Co-labeling with antibodies against calbindin and VGluT2 revealed that although fewer

VGluT2-containing CF terminals were present in mutant cerebellum, terminals that were present had correctly targeted Purkinje cell dendrites (Fig. 2R,S). To assess whether CFs ascended Purkinje cell dendrites in mutants, we examined whether CF terminals extended as far into the molecular layer as in controls. VGluT2-containing nerve terminals extended up through ~75% of the molecular layer in controls (Fig. 2T). Although fewer VGluT2-containing varicosities were observed in mutants, those varicosities present appeared through an equivalent percentage of the molecular layer (Fig. 2T). These two findings suggest that CFs were capable of targeting and "climbing" Purkinje cell dendrites in the absence of collagen XVIII/endostatin. However, to definitively assess their morphology, we anterogradely labeled CFs with lipophilic cyanine dye (DiI) in P20 mutants and controls (Fig. 2U,V). The average length of CF arbors and the proportion of molecular layer that they crossed were unaltered in *col18a1*$^{-/-}$ mutants (Fig. 2W,X). Taken together these studies reveal that reduced numbers of VGluT2-immunoreactive terminals did not result from altered Purkinje cell or CF morphology.

Endostatin induces climbing fiber terminal formation in vitro

To address whether Purkinje cell-derived endostatin was capable of inducing CF nerve terminal formation we generated dissociated cultures from the inferior olivary nucleus. Since cells in this nucleus do not express *col18a1* these cultures lack endogenous endostatin (Fig. S5). We therefore assessed whether the application of recombinant endostatin onto these neurons affected their CFs *in vitro*. Application of endostatin had no appreciable affect on the number or morphology of CF-generating inferior olivary neurons (data not shown), which were identified by their expression of calbindin (Calb) (Fig 3A). As we were interested in the axons (and not dendrites) of these neurons, we labeled axons with antibodies against neurofilament (NF) which predominantly labeled CF axons and not other cells in our cultures based on their co-expression of Calb (89.6% ± 2.1%[SD] of NF expressing neurons co-expressed Calb; N=4 experiments; n = 416 neurons)(Fig. 3B). Application of endostatin onto these cultures produced a robust increase in the clustering of VGluT2-immunoreactive terminals on NF-positive CFs (Fig. 3C-E,H). Importantly, the presence of endostatin *in vitro* had no significant affect on mRNA expression levels of *vglut2* (Fig. 3I), indicating that endostatin was not merely altering VGluT2 production. Moreover, endostatin-induced varicosities not only contained VGluT2, but also contained other synaptic vesicle associated proteins such as SV2 and synaptophysin (Syn)(Fig. 3F,G), suggesting they were indeed sites of neurotransmitter release (and not just sites of VGluT2 accumulation). Taken together, these results demonstrate that collagen XVIII/endostatin is not only necessary for CF terminal formation *in vivo*, but endostatin is sufficient to induce presynaptic differentiation of these terminals *in vitro*.

To test whether the ability of endostatin to induce presynaptic differentiation was specific to CF axons we repeated these experiments with dissociated granule cells. We failed to detect differences in the number of VGluT1-immunoreactive varicosities in the presence of recombinant endostatin (data not shown), suggesting that the ability of endostatin to induce presynaptic differentiation is cell-type specific.

Endostatin signals through α3β1 integrins to induce synaptic differentiation

We next explored what receptors might transduce these endostatin-induced signals in inferior olivary neurons. Outside of the nervous system, endostatin signals through αvβ3, αvβ5 and α5β1 integrin heterodimers (Ricard-Blum and Ballut 2011) – all of which are expressed in the inferior olive (Fig. S5E). More importantly, immunostaining for the β1 and β3 integrin subunits revealed both were present on CF axons *in vitro* (Fig. 4A,B; 99%±1% of NF-immunoreactive [NF-IR] axons contained β1 integrin, N=3 experiments, n=257 axons; 93%±3% of NF-IR axons contained β3 integrin, N=3, n=348). As the functions of β1

and β3-containing integrins are RGD-binding dependent, we tested whether endostatin-induced synaptogenesis could be blocked by RGD-containing peptides. Indeed, application of these peptides inhibited the ability of endostatin to induce CF terminal formation (Fig. 4F-H,K).

To determine which specific integrin heterodimer transduced endostatin-mediated signals, we explored the expression of the αv and α5 integrin subunits on CF axons. Surprisingly, neither was present on many CF axons (Fig. 4C,D; 1%±1% of NF-IR axons contained αv integrin, N=3, n=335; 6%±1% of NF-IR axons contained α5 integrin, N=3, n=271). We therefore explored other integrin α subunits that form heterodimers with β1 or β3 subunits. One interesting candidate was the α3 integrin subunit: α3β1 integrin (the only integrin containing the α3 subunit) binds in an RGD-dependent fashion (Akula et al. 2002), is present on nerve terminals (Cohen et al. 2000), and links synaptic cleft molecules to active zone components within the nerve terminal (Carlson et al. 2010). Here we show that nearly all CF axons contained α3 integrin (Fig. 4E, 99%±1% of NF-IR axons contained α3 integrin, N=3, n=335). The distribution of this integrin appeared evenly distributed throughout CF axons in control and endostatin-treated cultures (Fig 4E and data not shown). In addition to *in vitro* experiments, western blots revealed α3β1 integrins were enriched in cerebellar synaptosome fractions (Fig. 4N and S1D). To test whether endostatin signaled through α3β1 integrins in our assays, inferior olivary neurons were treated with function-blocking α3 integrin antibodies in conjunction with recombinant endostatin. Endostatin's ability to induce nerve terminal formation was abolished in the presence of these antibodies (Fig. 4I-K). Interestingly, and in contrast to CF axons, few axons from dissociated granule cells contained α3 integrins (although they did contain β1 integrins) (Fig. 4L,M; 5.2%±1% of NF-IR granule cell axons contained α3 integrin, N=6, n=256; 97.5%±0.9% of NF-IR axons contained β1 integrin, N=6, n=184). We suspect that differences in the expression of α3β1 integrins account for the cell-type specific function of endostatin.

Finally, since α3β1-endostatin interactions had not been reported previously, we confirmed their interaction by immunoprecipitating these integrin subunits from cerebellar and synaptosome extracts with endostatin antibodies (Fig. 4O). Surface plasmon resonance (SPR) binding assays were used to further demonstrate that α3β1 integrin directly binds endostatin with high affinity (K_D = 9.0 ± 3.6 nM, n=2). The interaction data were best fit by a two-state interaction model (data not shown), similar to the binding of endostatin to α5β1 and αvβ3 integrins that we previously reported (Faye et al. 2009). Thus, α3β1 integrin is a novel receptor for endostatin.

The mammalian cerebellum has become a well-studied model for identifying synapse-specific signals that regulate neural circuit formation (Umemori et al. 2004; Scheiffele et al. 2000; Matsuda et al. 2010; Ango et al. 2004; Kalinovsky et al. 2011). In this study we have added to our understanding of cerebellar circuit formation by identifying a matricryptin-releasing collagen that is necessary for the organization of climbing fiber terminals. While previous roles for collagen XVIII/endostatin have been described at the NMJ in worms, fish and flies, we found that despite its importance in cerebellum, collagen XVIII is dispensable for NMJ formation in mice (Fig. S6). In addition to being the first report of a matricryptin that regulates neural circuit formation in the mammalian brain, our studies also provide a cellular mechanism that may help explain why collagen XVIII-deficiency in Knobloch syndrome may predispose patients to neurological deficits (Suzuki et al. 2002).

EXPERIMENTAL PROCEDURES

Animals

Wild type mice were obtained from Charles River Laboratories (Wilmington, MA). Collagen XVIII null mice (*col18a1*$^{-/-}$) were described previously (Fukai et al. 2002). Standard rotarod experiments were performed on a Rotamex-5 (Columbus Instruments) (Shiotsuki et al. 2010) with a 3 cm rod. At the onset of experiments, rods rotated at 1rpm, however every 15 seconds the speed increased 1 rpm. The Rotamex-5 recorded the time at which each mouse fell. A total of 13 mutants and 10 littermate controls were analyzed. All analyses conformed to National Institutes of Health (NIH) guidelines and were carried out under protocols approved by the Virginia Commonwealth University (VCU) Institutional Animal Care and Use Committee.

Reverse Transcription-Polymerase Chain Reaction (RT-PCR)

RNA isolation, reverse transcription, PCR, and real-time quantitative PCR were all performed as previously described (Su et al. 2010). Primer sequences can be found in Supplemental Experimental Procedures.

Immunohistochemistry (IHC)

Fluorescent IHC was performed on 16 μm cryosectioned paraformaldehyde-fixed brain tissue or cultured neurons as described previously (Fox et al. 2007; Su et al 2010). Images were acquired on a Zeiss AxioImager A1 fluorescent microscope or a Leica SP2 confocal microscope. When comparing different ages of tissues or between genotypes, images were acquired with identical parameters. Tissues from at least 4 animals were analyzed for each genotype and IHC analysis was performed on at least random 8 fields (875 μm × 650 μm) per animal. Total number of puncta per field was counted manually. Average fluorescent intensities were measured in ImageJ as previously described (Su et al. 2010). A list of the antibodies and additional details can be found in Supplemental Experimental Procedures.

In situ Hybridization (ISH)

Riboprobe generation and *in situ* hybridization were performed as described previously (Su et al. 2010). Sense and antisense riboprobes against *col18a1* were generated from a 967-bp fragment of *col18a1* (corresponding to nucleotides 3190-4156) and were hydrolyzed to 500 nt.

Western blot (WB) and Immunoprecipitation (IP)

WBs and IPs were performed as described previously (Fox and Sanes 2007; Su et al. 2010). A previously described rabbit polyclonal antibody against endostatin was used for IPs (Faye et al. 2010). Additional information can be found in Supplemental Experimental Procedures.

In vitro cultures

Inferior olives (IO) were dissected from P0 mouse brains and were digested in 0.25% trypsin. Trypsin was inactivated and tissue was transferred to Neurobasal medium containing 0.5mM L-Glutamine, 25 uM L-Glutamate, 10ug/ml Gentamicin and 10% fetal bovine serum (FBS). Single cell suspensions were plated on poly-L-lysine treated chamber slides and were cultured for 4 days. After 2 additional days in Neurobasal medium containing 0.5mM L-Glutamine, 10ug/ml Gentamicin and B27 supplement, IO cells were treated with endostatin (0.1 ug/ml; ProSpec Inc.), BSA (0.1ug/ml), RGD (10uM), RAD (10uM), integrin α3 antibody (25ug/ml; Millipore) and/or mouse IgG (25ug/ml). After 2 days cells were fixed with 4% paraformaldehyde and immunostained. Granule cell cultures

were generated as previously described (Umemori et al. 2004) and were treated as described above.

Climbing fiber (CF) labeling

CF labeling was performed using the method of Kiyohara et al (2003). Brains were fixed in 4% PFA and DiI (0.5-1.0% in DMSO) was injected into the inferior cerebellar peduncle. Brains were incubated in 4% PFA at 37°C for 3 weeks, sectioned with a vibratome, and imaged with a Leica SP2 scanning confocal microscope. CF arbors and the extent of the molecular layer were measured in ImageJ.

SPR binding assays

The SPR binding assays were performed in a Biacore T200 instruments (GE Healthcare). Recombinant human endostatin was covalently immobilized to the dextran matrix of a CM5 sensor chip *via* its primary amine groups as described previously (Faye *et al.*, 2009). Sensorgrams collected on the control flow cell were automatically subtracted from the sensorgrams obtained on immobilized endostatin to yield specific binding responses. Kinetic and affinity constants were calculated by injecting several concentrations of α3β1 integrin (Millipore). Complexes were dissociated with 2 M NaCl. Rate constants were calculated using Biacore T200 software.

Supplementary Material

Refer to Web version on PubMed Central for supplementary material.

Acknowledgments

We thank Drs. J.R. Sanes, J.F. Strauss III, H. Umemori and G. Valdez for comments on the manuscript, Dr. Bjorn Olsen (Harvard) for *col18a1*$^{-/-}$ mice, R.Salza (University Lyon) for help with binding assays, and Christophe Quétard (GE Healthcare, France) for providing access to a Biacore T200 system. This work was supported by an A.D. Williams grant (MAF) and the National Institutes of Health (EY021222 to MAF). Microscopy was performed at the VCU Microscopy Facility supported by an NIH Core Grant (NS047463).

REFERENCES

Ackley BD, Kang SH, Crew JR, Suh C, Jin Y, Kramer JM. The basement membrane components nidogen and type XVIII collagen regulate organization of neuromuscular junctions in Caenorhabditis elegans. J Neurosci. 2003; 23:3577–3587. [PubMed: 12736328]

Akula SM, Pramod NP, Wang FZ, Chandran B. Integrin alpha3beta1 (CD 49c/29) is a cellular receptor for Kaposi's sarcoma-associated herpesvirus (KSHV/HHV-8) entry into the target cells. Cell. 2002; 108:407–419. [PubMed: 11853674]

Ango F, di Cristo G, Higashiyama H, Bennett V, Wu P, Huang ZJ. Ankyrin-based subcellular gradient of neurofascin, an immunoglobulin family protein, directs GABAergic innervation at Purkinje axon initial segment. Cell. 2004; 119:257–272. [PubMed: 15479642]

Carlson SS, Valdez G, Sanes JR. Presynaptic calcium channels and alpha3-integrins are complexed with synaptic cleft laminins, cytoskeletal elements and active zone components. J Neurochem. 2010; 115:654–666. [PubMed: 20731762]

Cohen MW, Hoffstrom BG, DeSimone DW. Active zones on motor nerve terminals contain alpha 3beta 1 integrin. J Neurosci. 2000; 20:4912–4921. [PubMed: 10864949]

Egles C, Claudepierre T, Manglapus MK, Champliaud MF, Brunken WJ, Hunter DD. Laminins containing the beta2 chain modulate the precise organization of CNS synapses. Mol Cell Neurosci. 2007; 34:288–298. [PubMed: 17189701]

Faye C, Moreau C, Chautard E, Jetne R, Fukai N, Ruggiero F, Humphries MJ, Olsen BR, Ricard-Blum S. Molecular interplay between endostatin, integrins, and heparan sulfate. J Biol Chem. 2009; 284:22029–22040. [PubMed: 19502598]

Faye C, Inforzato A, Bignon M, Hartmann DJ, Muller L, Ballut L, Olsen BR, Day AJ, Ricard-Blum S. Transglutaminase-2: a new endostatin partner in the extracellular matrix of endothelial cells. Biochem J. 2010; 427:467–475. [PubMed: 20156196]

Fox MA. Novel roles for collagens in wiring the vertebrate nervous system. Curr Opin Cell Biol. 2008; 20:508–513. [PubMed: 18573651]

Fox MA, Sanes JR. Synaptotagmin I and II are present in distinct subsets of central synapses. J Comp Neurol. 2007; 503:280–296. [PubMed: 17492637]

Fox MA, Sanes JR, Borza DB, Eswarakumar VP, Fassler R, Hudson BG, John SW, Ninomiya Y, Pedchenko V, Pfaff SL, et al. Distinct target-derived signals organize formation, maturation, and maintenance of motor nerve terminals. Cell. 2007; 129:179–193. [PubMed: 17418794]

Fox MA, Umemori H. Seeking long-term relationship: axon and target communicate to organize synaptic differentiation. J Neurochem. 2006; 97:1215–1231. [PubMed: 16638017]

Fremeau RT Jr. Troyer MD, Pahner I, Nygaard GO, Tran CH, Reimer RJ, Bellocchio EE, Fortin D, Storm-Mathisen J, Edwards RH. The expression of vesicular glutamate transporters defines two classes of excitatory synapse. Neuron. 2001; 31:247–260. [PubMed: 11502256]

Fukai N, Eklund L, Marneros AG, Oh SP, Keene DR, Tamarkin L, Niemela M, Ilves M, Li E, Pihlajaniemi T, Olsen BR. Lack of collagen XVIII/endostatin results in eye abnormalities. Embo J. 2002; 21:1535–1544. [PubMed: 11927538]

Kalinovsky A, Boukhtouche F, Blazeski R, Bornmann C, Suzuki N, Mason CA, Scheiffele P. Development of axon-target specificity of ponto-cerebellar afferents. PLoS Biol. 2011; 9:e1001013. [PubMed: 21346800]

Kiyohara Y, Endo K, Ide C, Mizoguchi A. A novel morphological technique to investigate a single climbing fibre synaptogenesis with a Purkinje cell in the developing mouse cerebellum: DiI injection into the inferior cerebellar peduncle. J Electron Microsc (Tokyo). 2003; 52:327–335. [PubMed: 12892223]

Ksiazek I, Burkhardt C, Lin S, Seddik R, Maj M, Bezakova G, Jucker M, Arber S, Caroni P, Sanes JR, et al. Synapse loss in cortex of agrin-deficient mice after genetic rescue of perinatal death. J Neurosci. 2007; 27:7183–7195. [PubMed: 17611272]

Mason CA, Gregory E. Postnatal maturation of cerebellar mossy and climbing fibers: transient expression of dual features on single axons. J Neurosci. 1984; 4:1715–1735. [PubMed: 6737039]

Matsuda K, Miura E, Miyazaki T, Kakegawa W, Emi K, Narumi S, Fukazawa Y, Ito-Ishida A, Kondo T, Shigemoto R, et al. Cbln1 is a ligand for an orphan glutamate receptor delta2, a bidirectional synapse organizer. Science. 2010; 328:363–368. [PubMed: 20395510]

Meyer F, Moussian B. Drosophila multiplexin (Dmp) modulates motor axon pathfinding accuracy. Dev Growth Differ. 2009; 51:483–498. [PubMed: 19469789]

Muragaki Y, Timmons S, Griffith CM, Oh SP, Fadel B, Quertermous T, Olsen BR. Mouse Col18a1 is expressed in a tissue-specific manner as three alternative variants and is localized in basement membrane zones. Proc Natl Acad Sci U S A. 1995; 92:8763–8767. [PubMed: 7568013]

Ricard-Blum S, Ballut L. Matricryptins derived from collagens and proteoglycans. Front Biosci. 2011; 16:674–697. [PubMed: 21196195]

Richter K, Langnaese K, Kreutz MR, Olias G, Zhai R, Scheich H, Garner CC, Gundelfinger ED. Presynaptic cytomatrix protein bassoon is localized at both excitatory and inhibitory synapses in rat brain. J Comp Neurol. 1999; 408(3):437–48. [PubMed: 10340516]

Sakimoto T, Kim TI, Ellenberg D, Fukai N, Jain S, Azar DT, Chang JH. Collagen XVIII and corneal reinnervation following keratectomy. FEBS Lett. 2008; 582:3674–3680. [PubMed: 18840438]

Scheiffele P, Fan J, Choih J, Fetter R, Serafini T. Neuroligin expressed in nonneuronal cells triggers presynaptic development in contacting axons. Cell. 2000; 101:657–669. [PubMed: 10892652]

Schneider VA, Granato M. The myotomal diwanka (lh3) glycosyltransferase and type XVIII collagen are critical for motor growth cone migration. Neuron. 2006; 50:683–695. [PubMed: 16731508]

Shiotsuki H, Yoshimi K, Shimo Y, Funayama M, Takamatsu Y, Ikeda K, Takahashi R, Kitazawa S, Hattori N. A rotarod test for evaluation of motor skill learning. J Neurosci Methods. 2010; 189:180–185. [PubMed: 20359499]

Sotelo C. Viewing the cerebellum through the eyes of Ramon Y Cajal. Cerebellum. 2008; 7:517–522. [PubMed: 18972180]

Su J, Gorse K, Ramirez F, Fox MA. Collagen XIX is expressed by interneurons and contributes to the formation of hippocampal synapses. J Comp Neurol. 2010; 518:229–253. [PubMed: 19937713]

Suzuki OT, Sertie AL, Der Kaloustian VM, Kok F, Carpenter M, Murray J, Czeizel AE, Kliemann SE, Rosemberg S, Monteiro M, et al. Molecular analysis of collagen XVIII reveals novel mutations, presence of a third isoform, and possible genetic heterogeneity in Knobloch syndrome. Am J Hum Genet. 2002; 71:1320–1329. [PubMed: 12415512]

Terauchi A, Johnson-Venkatesh EM, Toth AB, Javed D, Sutton MA, Umemori H. Distinct FGFs promote differentiation of excitatory and inhibitory synapses. Nature. 2010; 465:783–787. [PubMed: 20505669]

Umemori H, Linhoff MW, Ornitz DM, Sanes JR. FGF22 and its close relatives are presynaptic organizing molecules in the mammalian brain. Cell. 2004; 118:257–270. [PubMed: 15260994]

HIGHLIGHTS

1. Endostatin, a collagen XVIII-derived matricryptin, is generated by Purkinje cells
2. Proper organization of climbing fiber terminals require collagen XVIII/endostatin
3. Application of endostatin induces climbing fiber terminal formation *in vitro*
4. Endostatin binds and signals through α3β1 integrins

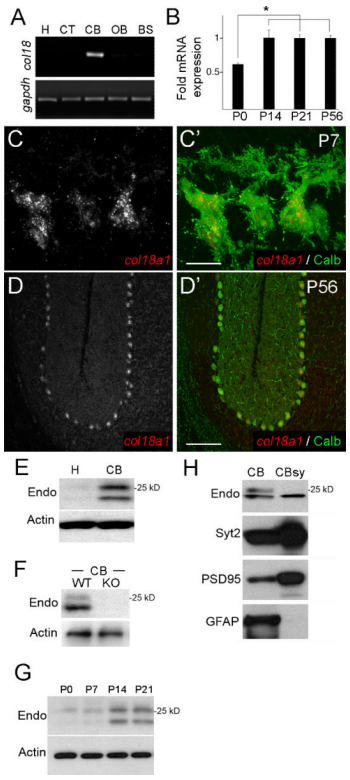

Figure 1. Expression of collagen XVIII/endostatin in mouse cerebellum

A. RT-PCR for *col18a1* and *gapdh* mRNAs from RNA isolated from P56 mouse hippocampus (H), cerebral cortex (CT), cerebellum (CB), olfactory bulb (OB), and brainstem (BS). **B.** qPCR show *col18a1* mRNA expression is developmentally regulated. Expression levels normalized to *gapdh*. Data shown are ± standard deviation (sd); n>3 per age. *Differ from P0 at P<0.003 by One-way analysis of variance (ANOVA). **C,D**. *In situ* hybridization show *col18a1* expression is restricted to Calbindin (Calb)-expressing Purkinje cells. **E.** Western blots demonstrate endostatin (endo)-containing fragments of collagen XVIII in P56 cerebellar protein extracts. **F.** Western blots of wild-type (WT) and *col18a1*$^{-/-}$ mutant (KO) CB extracts demonstrate antibody specificity. **G.** Western blots show levels of endostatin-containing peptides are developmentally regulated. Actin is a loading control for **E-G**. **H.** Western blots demonstrate a 20 kDa endostatin-containing fragment is present in cerebellar synaptosome fractions (CBsy). CBsy lack non-synaptic proteins, such as GFAP, and are enriched for synaptic proteins (eg. PSD95, Syt2). Scale bar in C = 15 μm and in D = 150 μm.

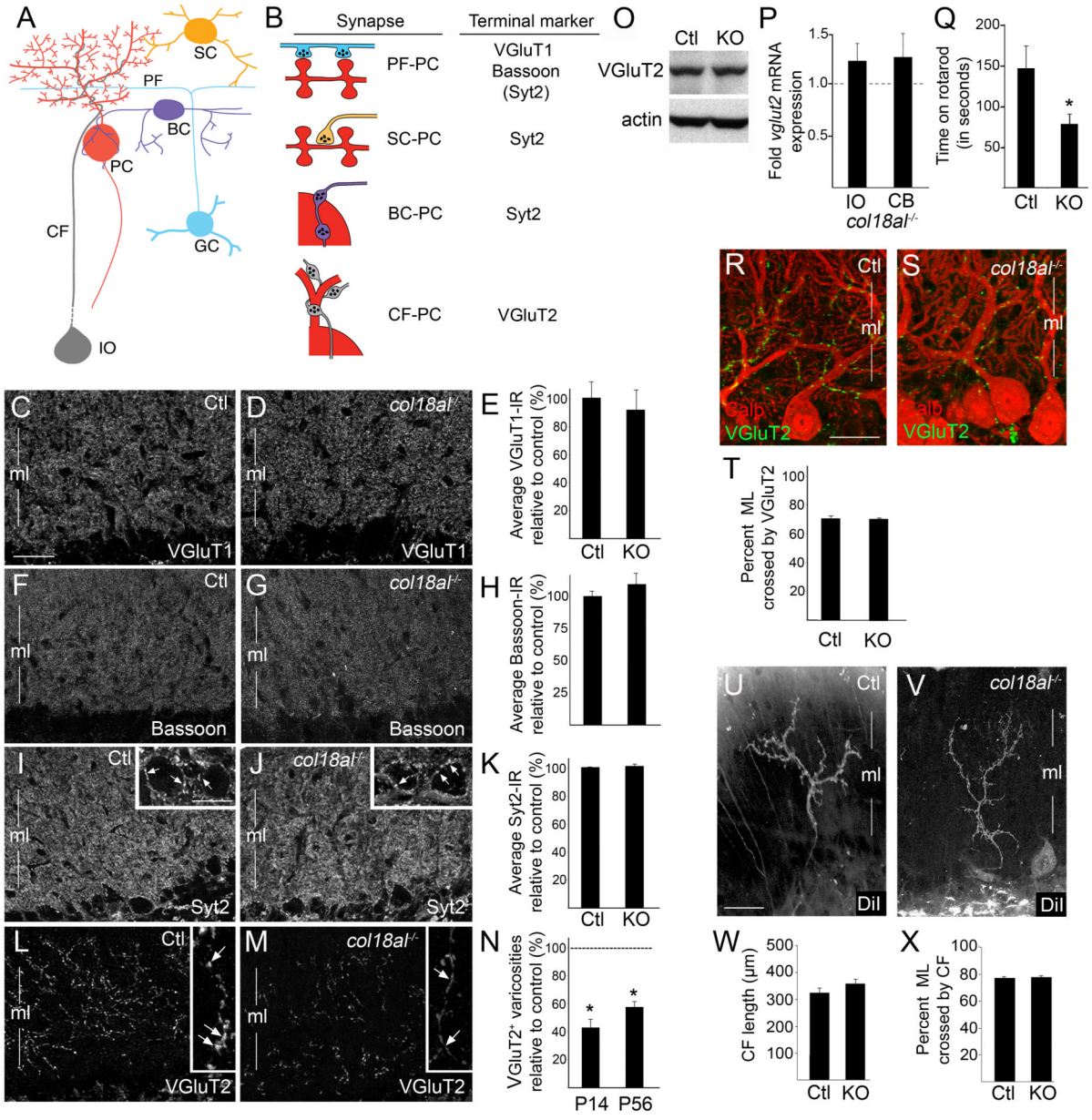

Figure 2. Collagen XVIII/endostatin is necessary for the organization of CF terminals

A. Neurons that synapse onto Purkinje cells (PC). BC – basket cell; CF – climbing fiber; GC – granule cell; IO – inferior olivary neuron; PF – parallel fiber; SC – stellate cell. **B**. Nerve terminal markers used to label terminals on PCs. Parentheses indicate Syt2 is present in a small set of PF terminals. **C,D,F,G,I,J,L,M**. Immunostaining for VGluT1 (**C,D**), Bassoon (**F,G**), Syt2 (**I,J**) and VGluT2 (**L,M**) in P56 control (Ctl) and *col18a1*$^{-/-}$ mutant cerebellum. Insets in **I,J** show high magnification of Syt2-positive axo-somatic terminals on PCs (see arrows). Insets in **L,M** show high magnification of VGluT2 distribution in CFs: note its diffuse axonal distribution in *col18a1*$^{-/-}$ mutants (arrows in **L,M**). **E,H,K**. Average fluorescent intensity of VGluT1-, Bassoon-, and Syt2-immunoreactivity in P56 control (Ctl) and mutants (KO). Data shown are mean ± SEM; n >4 mice per genotype. **N.** Quantification of the total number of VGluT2-positive varicosities per image field in P14 and P56 *col18a1*$^{-/-}$ mutants compared to controls (dashed line). Data shown are mean ± SD; n >4

mice per genotype. *Differ from litter mate controls at $p<0.001$ by Students t-test. **O.** Western blots show no difference in VGluT2 levels in P56 Ctl and KO cerebellum (CB). Actin was a loading control. **P.** qPCR of *vglut2* mRNA expression levels in P56 IO and CB of KOs and controls (dashed line). Data are mean ± SEM; n =3. **Q.** Adult KOs exhibit impaired mobility on a rotating rod. Data are mean ± SEM; n =10 Ctls and 13 KOs. *Differ from Ctls at $p<0.05$ by Tukey HSD Test for differences between means. **R,S.** Immunostaining for Calb and VGluT2 in P21 Ctl and KO cerebella. **T.** Quantification of the percent of ML crossed by VGluT2-containing nerve terminals. Data are mean ± SEM; n = 60 measures from 3 mice. **U,V**. DiI labeled climbing fibers in the ML of P20 control and *col18a1*$^{-/-}$ mutant cerebellum. **W**. CF length in ML of KO and Ctl cerebella. **X.** Quantification of the extent of ML crossed by the CFs in KO and Ctl cerebella. For **W,X** data are mean ± SEM; n = 26 control CFs and 23 mutants CFs. Scale bar in C = 30 μm for C,D,F,G,I,J,L,M, in insets = 18μm, in Q= 25 μm for Q,R, and in T = 30 μm for T,U.

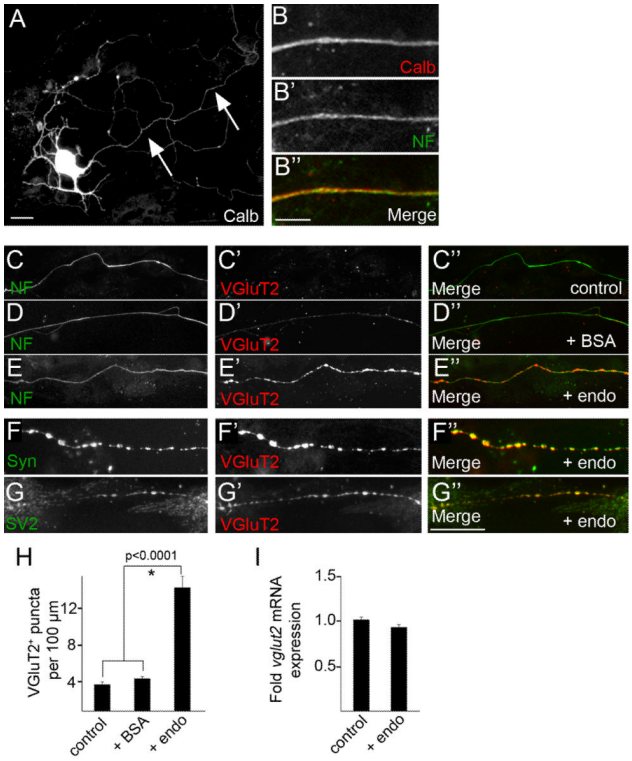

Figure 3. Endostatin induces CF terminal formation *in vitro*

A. Inferior olivary neuron labeled by Calb-IHC *in vitro*. Arrows indicate CF axon. **B**. CF axons were labeled by neurofilament (NF)-IHC. **C-E.** Control or BSA-treated CF axons had few VGluT2-immunoreactive synaptic varicosities, however treatment with 0.1 μg/ml endostatin (endo) induced varicosity formation. **F,G.** Endostatin-induced VGluT2-positive varicosities contained other nerve terminal associated proteins, i.e. synaptophysin (Syn; **F**) and SV2 (**G**). **H.** Quantification of VGluT2-positive synaptic varicosities in control and treated cultures. Data shown are ± SD: n>4 experiments in quadruplicate. *Differ from control cultures at p<0.0001 by Tukey-Kramer Test for Differences Between Means. **I.** qPCR revealed that endo did not significantly alter *vglut2* mRNA expression. Expression levels normalized to *gapdh*. Data shown are ± SD; n>3. Scale bar in A = 25 μm, in B = 8 μm and in E = 25 μm for C-E.

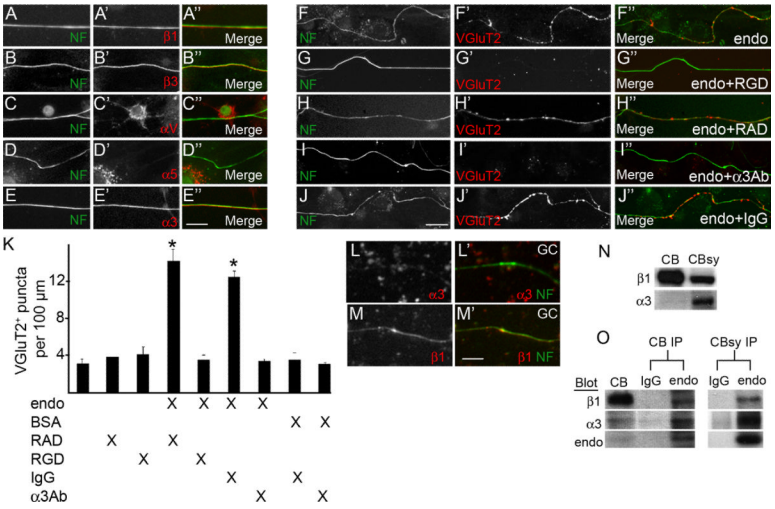

Figure 4. Endostatin signals through α3β1 integrins to induce nerve terminal formation

A-E. IHC revealed that the β1, β3, and β3 integrin subunits were present on NF-positive CF axons *in vitro*. **F-J.** Endostatin's ability to induce the formation of VGluT2-positive synaptic varicosities was inhibited by the application of 10 mM RGD peptides (**G**) or 25μg/ml anti-α3 integrin antibodies (**I**), but not by control peptides (RAD; **H**) or antibodies (IgG; **J**). **K.** Quantification of VGluT2-positive synaptic varicosities in cultures treated with combinations of endo, BSA, RAD peptides, RGD peptides, control IgG antibodies and anti-α3 integrin antibodies. Data shown are ± sd: n>4 experiments in quadruplicate. *Cultures treated with endo and either control peptides / antibodies differ from all other treatment groups at $p<0.0001$ by Tukey-Kramer Test for Differences Between Means. **L,M.** IHC revealed β1, but not α3, integrin subunits were present on cultured granule cell (GC) axons. **N.** Western blots demonstrate the presence of the α3 and β1 integrin subunits in cerebellar extracts (CB) and cerebellar synaptosomes (CBsy). **O.** Endostatin-antibodies immunoprecipitated the α3 and β1 integrin subunits from both CB and CBsy. Scale bar in E = 20 μm for A-E, in J = 25 μm for F-J, and in M = 15 μm for L,M.